

Improving Plasma Actuator Thrust at Low Pressure Through Geometric Variation

Paul D. Friz* and Joshua L. Rovey†

Missouri University of Science and Technology, Rolla, Missouri, 65409, USA

The force production and power consumption of plasma actuators with varying electrode geometries was measured. The geometries were varied by changing the length of the exposed and buried electrodes as well as varying the chord-wise gap between the electrodes. Each actuator was driven with a 5 kHz sine wave at 16 kVpp, and operated at pressures ranging from 10-101 kPa, which corresponds to altitudes from 16,000 m to sea level. The electric field of each configuration was also modeled using Maxwell Ansoft. Increasing the length of the buried electrode was found to have the greatest effect on thrust production especially at low pressure. Actuators with 75 mm buried electrodes produced an average of 26% more thrust at all pressures and 34% more thrust at 20-40 kPa than the traditional 15 mm buried electrode. The gap study revealed that actuators with a 1 mm gap produced the most force at all pressures. All actuator designs were found to have a similar linear relationship between their effectivenesses and operating pressure.

Nomenclature

a	Chord-wise exposed electrode length, mm
b	Chord-wise buried electrode length, mm
c	Chord-wise gap between exposed and buried electrodes, mm
t	Thickness of dielectric material, mm
p	Pressure, kPa
F	Force, mN
P	Power, W
V	Voltage, kVpp
I	Current, mA
ξ	Effectiveness, $\frac{mN}{W}$

I. Introduction

SINGLE dielectric barrier discharge (SDBD) plasma actuators are a promising flow control device for a variety of aerospace applications. Applications of plasma actuators include: reduction of flow separation on airfoils at high angle of attack,¹ separation control on turbine blades,² controlling Micro and Unmanned Aerial Vehicles (μ AVs) and (UAVs)³ and control of the phantom yaw experienced by missile bodies at high angle of attack. The main advantage of plasma actuators over traditional flow control devices is that they have no moving parts and can be turned on and off almost instantaneously.⁴

A SDBD plasma actuator consists of two electrodes separated by a dielectric in an asymmetric configuration shown in Figure 1. The electrodes are usually copper or aluminum tape placed directly on the dielectric. Common dielectrics include but are not limited to Teflon, Kapton, fiberglass epoxy, and Macor.⁵⁻⁷ The buried electrode is electrically grounded and encapsulated in a second dielectric. In this and many other studies Kapton tape is used as the dielectric material to encapsulate the buried electrode thus preventing

*Graduate Research Assistant, Department of Mechanical and Aerospace Engineering, 160 Toomey Hall, 400 West 13th Street, Student Member AIAA

†Assistant Professor of Aerospace Engineering, Department of Mechanical and Aerospace Engineering, 292D Toomey Hall, 400 West 13th Street, Senior Member AIAA

electrical discharge and plasma formation on the back side of the actuator. The exposed electrode is typically driven by an AC waveform of 1-15 kHz and 12-20 kVpp⁵⁻⁹. The AC cycle of the actuator is commonly divided into two sections; the forward stroke, when the voltage on the exposed electrode is negative going, and the backward stroke, when the voltage is positive going. During the forward stroke the electrons coming off the exposed electrode collide with neutral air particles ionizing them. Those ions are then accelerated away from the exposed electrode and collide with the surrounding air thus inducing what is called ionic wind. During the backward stroke electrons return to the exposed electrode coming off the dielectric surface, again colliding with air particles creating plasma.^{7,10} It has been shown that 97% of the momentum coupling between the plasma and air occurs during the forward stroke and that negative oxygen ions are primarily responsible for the momentum transfer.¹¹ Because time resolved measurements of the actuator force production are difficult to obtain it is still not clear if the plasma actuator pushes ions away in both the forward and backward stroke or if it pushes ions during the forward stroke but weakly pulls ions back during the backward stroke.¹¹

If plasma actuators are to be used on aircraft and missiles they must first be demonstrated to be capable of producing enough thrust to provide control at the low pressures found at high altitudes. Abe *et al.* demonstrated that for a plasma actuator with exposed and buried electrode lengths of 15 mm separated by fiberglass epoxy and a 1mm chord-wise gap as pressure decreases the thrust production of the plasma actuator increases slightly. However, as pressure is decreased beyond 75 kPa, thrust production decreases significantly.⁶ Nichols measured the electric field of an actuator with a 50 mm buried electrode and showed that at low pressure up to 88% of the plasma is formed in regions where the electric field is relatively weak.⁷ A more recent study by Soni and Roy showed that the force vs pressure profile as well as the effectiveness (defined as unit of thrust produced per unit of power used) can be modified by changing the dielectric material, dielectric thickness, and applied voltage. Specifically they found that thrust is increased with decreasing dielectric thickness and that decreasing dielectric thickness pushes the peak of the force vs pressure profile to lower pressures.⁵

The rest of this paper is divided into three main sections: Experimental Setup, Results, and Discussion. The Results and Discussion sections are each divided into three subsections examining the effects of varying buried electrode length, exposed electrode length, and the chord-wise gap length.

II. Experimental Setup

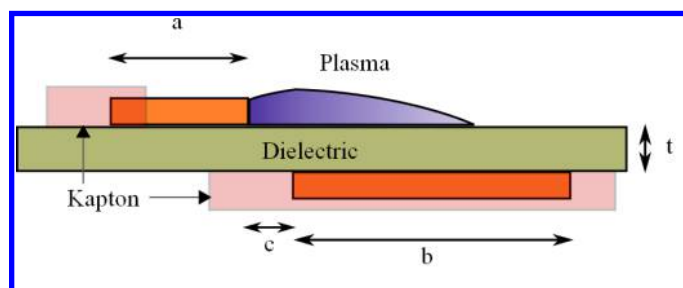


Figure 1. Plasma actuator design used in this study. The lengths a , b , and c were independently varied.

The plasma actuator design used in the experiment is shown in Figure 1. The insulating dielectric has a thickness $t=1.54$ mm, and is made of G-10 glass epoxy with dielectric constant $\epsilon_r = 4.9$. The electrodes are made of .04 mm thick copper tape spanning 240 mm and are placed on either side of the dielectric and separated by a gap of $c = 1$ mm. The chord length of the exposed and buried electrodes vary and are denoted a and b respectively. The exposed electrode is driven with a 5 kHz 16 kVpp sinusoidal electrical signal, and its upstream edge is covered in Kapton tape to prevent any reverse discharges. The buried electrode is electrically grounded and is completely covered in multi-layered Kapton tape to prevent electrical discharge. A Rigol DG1022 function generator provides the 5 kHz sinusoidal signal. The signal is then amplified by a Crown CE 2000 amplifier and sent to a Corona Magnetics CMI-5525-2 transformer. The voltage and current output from the transformer is monitored by a North Star PVM-5 high voltage probe and a Pearson Electronics model 4100 current monitor. A high voltage line carries the now 5 kHz 16 kVpp signal from the output of the transformer into the vacuum chamber. A lightly insulated 0.25 mm diameter wire goes from the high voltage

wire to the exposed electrode of the plasma actuator so that the heavy high voltage wire does not interfere with force measurements. A similar wire grounds the buried electrode to the vacuum chamber which is in turn grounded to the building. The vacuum chamber has an inner diameter and length of 0.60 m and 0.70 m respectively. The pressure within the chamber is monitored by a Kurt J. Lesker KJL275800 thermocouple gauge. The KJL275800 is accurate to $\pm 2.5\%$ above 50 kPa, below 50 kPa it is only accurate to $\pm 10\%$. For the sake of clarity pressure error bars are omitted on all graphs in this report. The plasma actuator is placed on an acrylic stand on a Torbal AGC500 scale. Traditionally plasma actuators are mounted in such a way that the plasma discharge points down. However, it was found that when the actuators were mounted in this fashion the acrylic stand blocked some of the ionic wind causing inaccurate measurements. To solve this the actuators were mounted upside down so that they were discharging up. Force measurements were obtained by averaging two sets of ten measurements taken over ten seconds from the scale and the errors reported are the standard deviation of those measurements. The current and voltage readings were acquired using a Tektronix DPO 2024 oscilloscope. The current and voltage waveforms were multiplied and averaged by the oscilloscope to obtain the average power measurements. The power measurements were found to vary by $\pm 10\%$ for any given pressure and driving voltage.

III. Results

To confirm the accuracy of the force measurements a plasma actuator matching the design of Abe *et al.* was constructed. The only differences between the two were that the new actuator dielectric had a thickness of 1.54 mm as opposed to Abe's, which was 1.80 mm thick and the electrodes spanned only 240 mm whereas Abe's spanned 300 mm. The actuator was driven at 5 kHz 20 kVpp and its Thrust/Length was found to be consistent with the measurements of Abe *et al.* and Soni and Roy (Figure 2). Soni and Roy reported that decreasing the thickness of the actuator dielectric increases its thrust production which accounts for why the force measurements of Soni and Roy, and those obtained in this experiment were on average 18% and 12% higher than that of Abe, respectively.^{5,6}

The results of this geometry study are divided into three sections, each showing how varying one geometric parameter affects actuator force production and effectiveness. In the following section the actuator buried electrode length, exposed electrode length and chord-wise gap length is varied respectively.

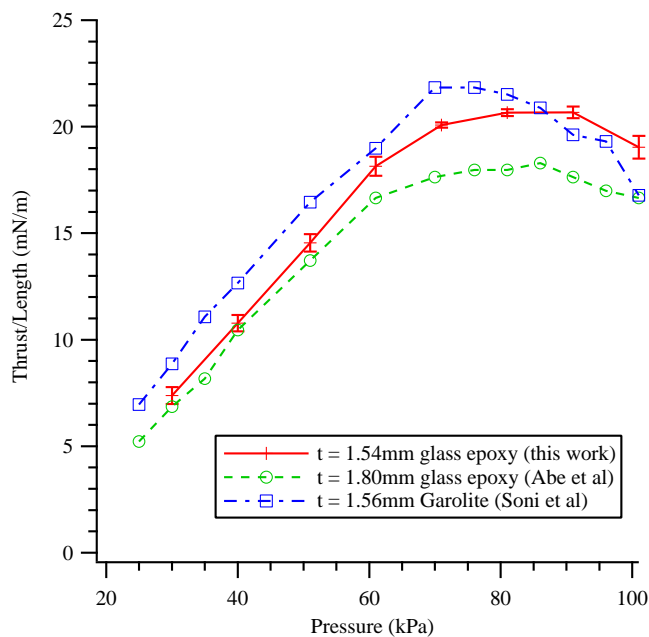


Figure 2. Replication of the results of Abe and Soni.

A. Buried Electrode Study

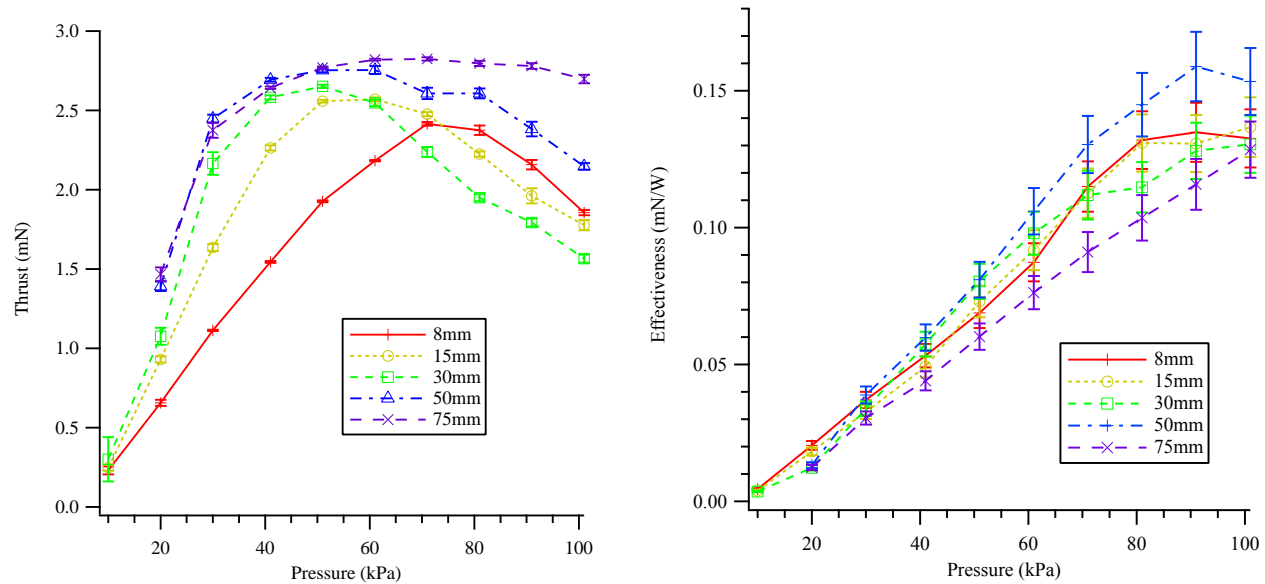


Figure 3. Force and effectiveness profiles of actuators with different buried electrode lengths.

In this study the electric field and capacitive effects of the plasma actuator were altered by changing the chord-wise length of the buried electrode. Five separate plasma actuators were constructed with 15 mm exposed electrodes and buried electrodes measuring $b = 8$ mm, 15 mm, 30 mm, 50 mm, and 75 mm. Each actuator had a 1mm chord-wise gap between the exposed and buried electrodes. The exposed electrode was driven at 5 kHz, 16 kVpp. The force and effectiveness profiles are shown in Figure 3. Initially as buried electrode length increases the thrust production at low pressures increases but decreases at higher pressures. However, as the buried electrode length is extended to 50 mm and beyond production is increased at all pressures. The 75 mm buried electrode actuator produced an average of 26% more thrust at all pressures and 34% more thrust at 20-40 kPa than the traditional 15 mm buried electrode actuator. No clear relationship between buried electrode length and the effectiveness profile is apparent however the $b = 50$ mm actuator was the most effective at all pressures and the $b = 75$ mm actuator was the least effective.

B. Exposed Electrode Study

In this study the force and effectiveness profiles were obtained for actuators with exposed electrodes of length $a = 10$ mm, 15 mm, and 20 mm. To ensure consistency the test was conducted on actuators with buried electrodes of length $b = 15$ mm and 75 mm. Again the actuators were driven at 5 kHz, 16 kVpp. The results in Figure 4 show that altering the exposed electrode length has little effect. At high pressures the $a = 15$ mm and $a = 10$ mm electrode force and effectiveness profiles are nearly identical as seen in Figure 4a and b. While increasing the exposed electrode length from $a = 15$ mm to $a = 20$ mm decreases average thrust production above 60 kPa by 13% and average effectiveness by 11%. At 70 kPa and below exposed electrode length does not effect thrust production for actuators with $b = 75$ mm. However, at 80kPa and above the $a = 15$ mm produced on average 8% and 16% more thrust than the $a = 20$ mm and $a = 10$ mm actuators respectively. Exposed electrode length had no noticeable effect on effectiveness for $b = 75$ mm actuators.

C. Gap Study

In this study two actuators with exposed electrodes $a = 15$ mm and buried electrodes $b = 15$ mm and $b = 75$ mm were studied. Force and effectiveness profiles were obtained for chord-wise gaps of $c = -3$ mm, 1 mm, and 3 mm. All other parameters remained the same as in the buried and exposed electrode studies. Figure 5a and c shows that changing the gap length from $c = 1$ mm to $c = -3$ or 3mm decreases force production for both the $b = 75$ mm and 15 mm actuators. On average for buried electrode length $b = 75$ mm the $c = -3$ mm and 3mm produced 10% less force than the $c = 1$ mm actuator. For the $b = 15$ mm actuator the $c = -3$

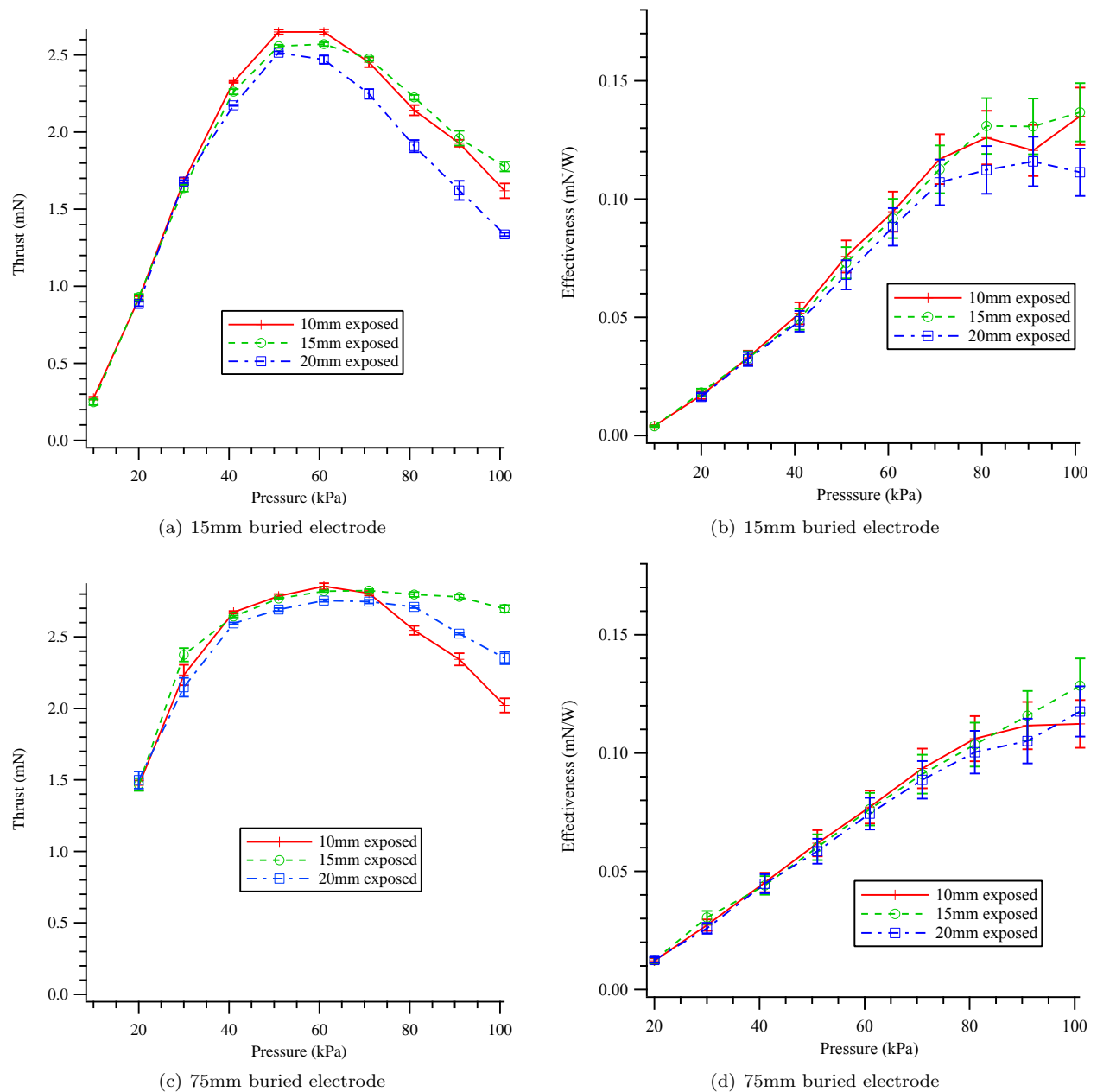


Figure 4. Force and effectiveness profiles of actuators with different exposed electrode lengths.

mm design produced 12% less thrust and the $c = 3$ mm design produced 9% less thrust on average than the $c = 1$ mm design. Altering chord-wise gap had little effect on the effectiveness of the actuators, however, the $b = 15$ mm $c = 3$ mm design was overall 13% more effective and was 22% more effective at 70 kPa and above, as seen in Figure 5b.

IV. Discussion

The overall trends and the effects of altering electrode geometry on the electric field, force production and effectiveness are discussed in this section. The electric field of each actuator was computed using the finite element analysis software Maxwell Ansoft. The electric field plotted is only the electric field due to the voltage of the exposed electrode and the effects of the dielectric materials and buried electrode. They do not show the effects on the electric field due to charge buildup on the dielectric surface during discharge or the

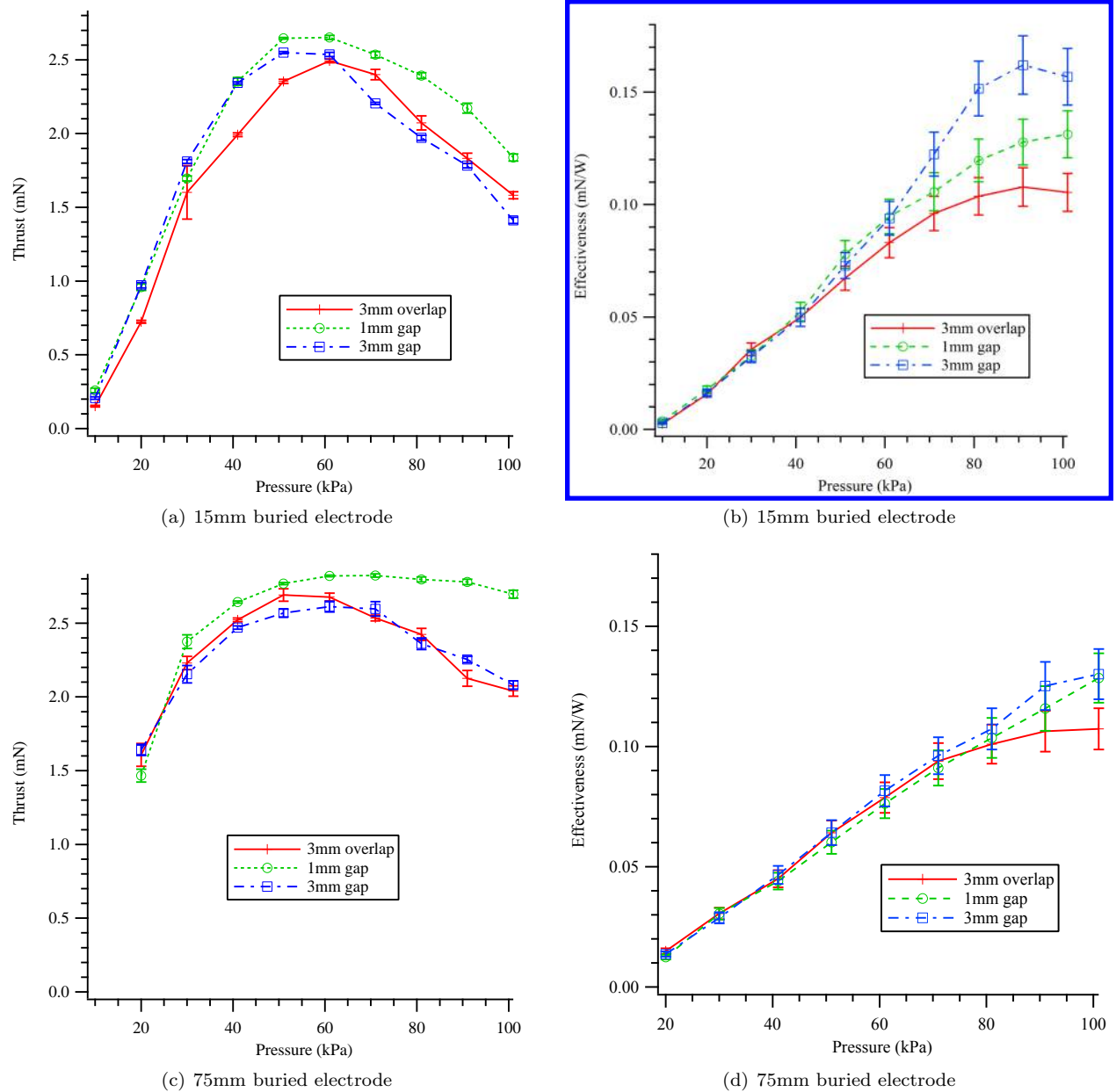
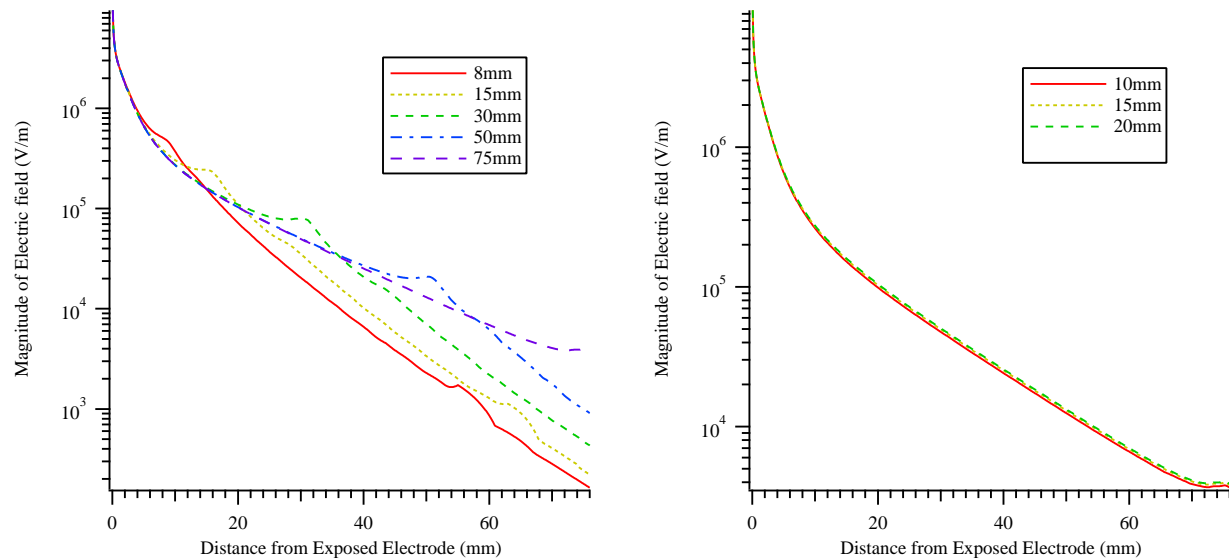


Figure 5. Force and effectiveness profiles of actuators with different gaps between their electrode.

effects of the plasma. Previous studies have shown that both the electric field and the charge distribution on the dielectric play key rolls in producing plasma and thrust.^{7,10}

A. Effects of Varying Buried Electrode Length

It was expected that actuators with longer buried electrodes would produce more thrust at lower pressures since the electric field can maintain a greater magnitude farther downstream as seen in Figure 6a. Figure 6a also shows that each actuator has the same magnitude of electric field up until the point where it reaches the end of its buried electrode at which point the electric field rises slightly then quickly falls off. Figure 7 shows the extent of the plasma formation as pressure decreases for actuators being driven at 16 kVpp with buried electrode lengths of $b = 8$ mm, 15 mm and 50 mm. Abe *et al.* and Soni and Roy separately demonstrated that as pressure is decreased the extent of the plasma over the buried electrode increases and that the extent of the plasma is limited to the length of the buried electrode.^{5,6} Figure 7 further illustrates those



(a) Electric field magnitude as buried electrode length is varied.

(b) Electric field magnitude as exposed electrode length is varied.

Figure 6. The various electric fields just above the surface of the dielectric as a function of distance downstream from the buried electrode as buried electrode length and chord-wise gap are changed.

findings and shows that until the pressure reaches 50kPa the primary factor limiting thrust production at low pressure is the extent of the plasma. Figure 3 shows that when the $b = 8\text{mm}$ actuator is driven at 16 kVpp it produces its maximum thrust at 70 kPa. As pressure decreases beyond 70 kPa the thrust production falls off quickly. In Figure 7b, which corresponds to $b = 8\text{ mm}$, and $p = 70\text{ kPa}$, the plasma has extended approximately 6mm downstream from the exposed electrode. 6 mm downstream of the exposed electrode is where the edge effects of the buried electrode can first be seen in Figure 6a. Similarly as seen in Figure 3 the $b = 15\text{ mm}$ actuator reaches its maximum force production at $p = 50 - 60\text{ kPa}$. At 50 kPa the plasma has extended approximately 11mm as seen in Figure 7g which also corresponds to the point on Figure 6a where the electric field starts to be effected by the edge of the buried electrode. Figure 3 also shows that the $b = 50\text{ mm}$ actuator has its thrust maximum at 50 kPa, its plasma extends much farther at lower pressures as seen in Figure 7l. Below 50 kPa the thrust production decreases but not nearly as fast as with actuators with shorter buried electrodes. The previous study by Nichols measuring the combined electric fields of both the electrodes and the charge distribution on the surface of the dielectric using V-dot probes, predicted that an actuator with a 50 mm buried electrode would produce the most force at 57 kPa and follow the general trends seen in Figure 3.⁷

Soni and Roy reported that as pressure decreases the effectiveness of actuators initially increases reaching a maximum at sub-atmospheric pressures then rapidly falls off as the pressure decreases further. However, the effectiveness profiles shown in Figure 3 linearly decrease as pressure is decreased in accordance with the previous study by Gregory *et.al.*¹² However, Soni and Roy operated their actuators at 6-15 kVpp and their results indicated that actuator maximum effectiveness occurs at higher pressures as driving voltage is increased.⁵ The $b = 8$ and $b = 50\text{ mm}$ actuators in Figure 3 reach a maximum effectiveness at 90 kPa. This implies that if the pressure were increased above atmospheric pressure that the effectiveness would cease to follow the increasing linear trend and decrease.

B. Effects of Varying Exposed Electrode Length

The maxwell analysis showed no significant difference in electric field when altering the exposed electrode length as seen in Figure 6b. This explains why changing the exposed electrode length has no large effect on thrust or effectiveness profiles.

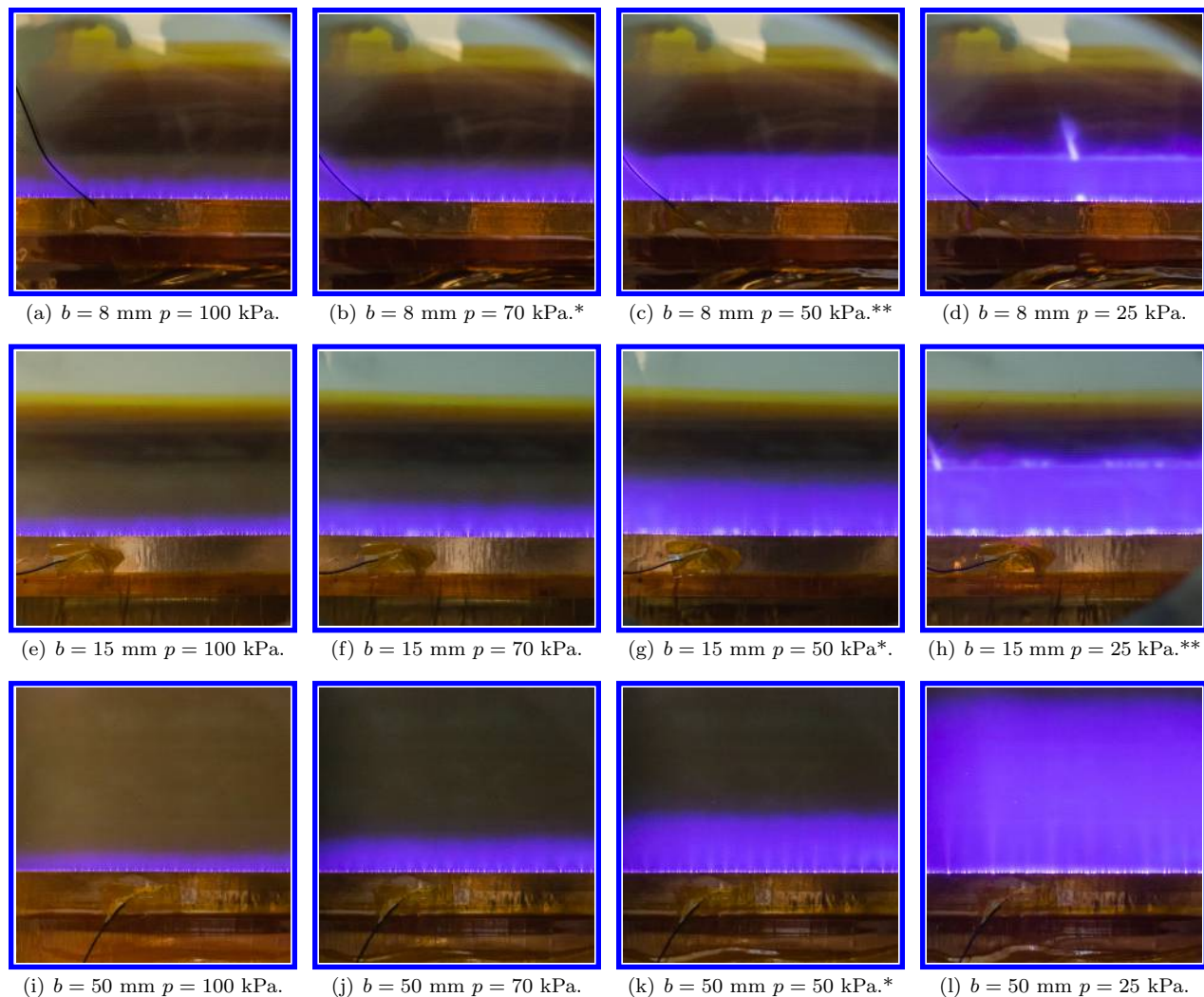


Figure 7. Plasma extent at 16 kVpp and varying pressure for plasma actuators with exposed electrode length 15 mm and buried electrode lengths of 8 mm, 15 mm and 50mm. The plasma brightens at the edge of the buried electrode outlining it as seen in (d) and (h).

***Pressure at which force production reaches maximum.**

****Pressure at which plasma extent becomes limited by buried electrode length**

V. Conclusion

Low pressure performance of SDBD plasma actuators was investigated at pressures ranging from 10-101 kPa. The effects of buried, and exposed electrode length, as well as chord-wise gap, on actuator thrust production and effectiveness were studied. As buried electrode length is increased the electric field extends farther down stream, and force production at high pressure initially decreases, but increases at low pressure. However, as buried electrode length is increased further thrust production increases at all pressures. Altering the length of the exposed electrode and chord-wise gap does not have as large of an effect on force production except at high pressures where actuators with $a = 15 \text{ mm}$ and $c = 1 \text{ mm}$ produced the most thrust. While altering the exposed electrode length and chord-wise gap did not improve thrust production increasing the chord-wise gap did improve actuator effectiveness. At 70 kPa and above an actuator with $a = 15 \text{ mm}$, $b = 15 \text{ mm}$, and $c = 3 \text{ mm}$ was on average 22% more effective than the original design of $c = 1 \text{ mm}$. All the actuators studied in this experiment exhibited a nearly linear relationship between effectiveness and operating pressure. The most effective actuator studied had a buried electrode of 50 mm and exposed electrode of 15 mm with a 1 mm gap, on average over all pressures it was 14% more effective than the original $b = 15 \text{ mm}$ design. The actuator which produced the most thrust overall had a buried electrode length of $b = 75 \text{ mm}$. It produced

26% more thrust at all pressures than the original $b = 15$ mm design and produced 34% more thrust between the pressures of 20 – 40 kPa. The long buried electrode plasma actuator designs presented in this paper will offer more aerodynamic control force to aircraft in low pressure environments.

VI. Acknowledgments

The authors wish to thank Lockheed Martin Missile and Fire Control for funding this work, and Crown Audio for donating the amplifier.

References

- ¹Moreau, E., “Airflow control by non-thermal plasma actuators.” *Journal of Physics D: Applied Physics*, Vol. 40, 2007, pp. 605–636.
- ²Ramakumar, K. and Jacob, J., “Flow Control and Lift Enhancement Using Plasma Actuators.” *AIAA Fluid Dynamics Conference and Exhibit*, AIAA, Paper 2005–4635, Toronto, Ontario Canada, 2005.
- ³Santhanakrishnan, A., Pern, N. J., Ramakumar, K., Simpson, A., and Jacob, J. D., “Enabling Flow Control Technology for Low Speed UAVs,” *AIAA Infotech@Aerospace*, AIAA, Paper 2005–6960, Arlington, Virginia, Sept. 2005.
- ⁴Corke, T. C., Enloe, C. L., and P. Wilkinson, S., “Dielectric Barrier Discharge Plasma Actuators for Flow Control,” *Annual Review of Fluid Mechanics*, Vol. 42, 2010, pp. 505–529.
- ⁵Soni, J. and Roy, S., “Low Pressure Characterization of Dielectric Barrier Discharge Actuators.” *Applied Physics Letters*, Vol. 102, No. 112908, 2013, pp. 1–5.
- ⁶Abe, T., Takizawa, Y., Sato, S., and Kimura, N., “Experimental Study for Momentum Transfer in a Dielectric Barrier Discharge Plasma Actuator.” *AIAA*, Vol. 46, No. 9, 2008, pp. 2248–2256.
- ⁷Nichols, T. G. and Rovey, J. L., “Surface Potential and Electric Field Measurements in Plasma Actuators at Low Pressure.” *AIAA*, Vol. 51, No. 5, 2013, pp. 1054–1065.
- ⁸Enloe, C. L., McLaughlin, T. E., VanDyken, R. D., Kachner, K. D., Jumper, E. J., and Corke, T. C., “Mechanisms and Responses of a Single Dielectric Barrier Plasma Actuator: Plasma Morphology.” *AIAA*, Vol. 42, No. 3, 2004, pp. 589–594.
- ⁹Enloe, C. L., McLaughlin, T. E., VanDyken, R. D., Kachner, K. D., Jumper, E. J., Corke, T. C., Post, M., and Haddad, O., “Mechanisms and Responses of a Single Dielectric Barrier Plasma Actuator: Geometric Effects.” *AIAA*, Vol. 42, No. 3, 2004, pp. 595–604.
- ¹⁰Enloe, C. L., Font, G., McLaughlin, T. E., and Orlov, D. M., “Surface Potential and Longitudinal Electric Field Measurements in the Aerodynamic Plasma Actuator,” *AIAA*, Vol. 46, No. 11, 2008, pp. 2730–2739.
- ¹¹Enloe, C. L., McHarg, M. G., and McLaughlin, T. E., “Time-correlated force production measurements of the dielectric barrier discharge plasma aerodynamic actuator,” *Journal of Physics D: Applied Physics*, Vol. 103, 2008.
- ¹²Gregory, J. W., Enloe, C. L., Font, G. I., and McLaughlin, T. E., “Force Production Mechanisms of a Dielectric-Barrier Discharge Plasma Actuator.” *45th AIAA Aerospace Sciences Meeting and Exhibit*, AIAA, Paper 2007-185, Reno, Nevada, 2007.